Available online at www.sciencedirect.com
ScienceDirect
Dyes and Pigments 77 (2008) 129−136
DYES and PIGMENTS
www.elsevier.com/locate/dyepig

The preparation and characterization of a graphite−PTFE cathode system for the decolorization of C.I. Acid Red 2

Minghua Zhou [a,b,*], Qinghong Yu [a], Lecheng Lei [a]

[a] *Department of Environmental Science, Zhejiang University, Hangzhou 310028, China*
[b] *Department of Chemical Engineering, Sydney University, NSW 2006, Australia*

Received 19 January 2007; received in revised form 20 April 2007; accepted 24 April 2007

Abstract

An undivided electrochemical system was used to produce hydrogen peroxide on a graphite−polytetrafluoroethylene cathode. Key factors for cathode preparation, electrochemical activity as well as cathode stability were investigated. The current efficiency for hydrogen peroxide production was ∼61−78% over a wide pH range (3−11) which decayed insignificantly after 10 times reuse. The influence of Na_2SO_4, pH, cathodic potential, initial dye concentration and ferrous ion concentration on decolorization were systematically studied. The results show that the presence of ferrous ion improved color removal greatly; at 0.2 mM Fe^{2+} almost 80% of the dye could be removed after 20 min, indicating that the electro-Fenton process offers promise for dye removal.

Keywords: Graphite−PTFE cathode preparation; Electro-generated H_2O_2; Azo dye treatment; Methyl red; Electro-Fenton; Decolorization

1. Introduction

In recent years electrochemical technologies have been extensively studied for water and waste water treatment due to their high efficiency, convenience and environmental compatibility [1−4]. Besides direct electrochemical oxidation, indirect electrochemical treatment via generation of hydrogen peroxide has also attracted interest as this environmentally friendly approach leaves no hazardous residues at the end of oxidation [5,6]. Hydrogen peroxide can be generated by the two-electron reduction of oxygen at an appropriate cathodic potential using, for example, graphite and gas diffusion electrodes, which overcome the drawback of conventional H_2O_2 transportation and its reaction activity decline [7,8]:

$$O_2 + 2H^+ + 2e^- \rightarrow H_2O_2 \qquad (1)$$

The major concern with this system relates to the improvement of hydrogen peroxide production; in this context, numerous efforts have been made, utilizing different cathodes and electrochemical systems. Alvarez-Gallegos and Pletcher adopted a reticulated vitreous carbon cathode to generate H_2O_2 in a divided system using a relatively expensive membrane, which could restrict its practical application in waste water treatment. While the current efficiency was concluded to be 40−70% at pH ∼ 2, this was not a function of either potential or catholyte composition [5]. Brillas et al. investigated H_2O_2 production using a gas diffusion cathode at pH 10.1−12.7 and found that current efficiency was influenced by current intensity, achieving a maximum value of only 46% [8]. Qiang et al. attempted the electrochemical generation of hydrogen peroxide on graphite in an acidic medium [6]. These workers obtained highest current efficiency at pH 2, although this dropped significantly even at slightly elevated pH values of 2.5−3.5, which were supposed to be the optimal pH range for advanced oxidation processes (AOPs) such as Fenton

---

[*] Corresponding author. Department of Environmental Science, Zhejiang University, Hangzhou 310028, China. Tel.: +86 571 88273090; fax: +86 571 88273693.

E-mail address: skynumen@yahoo.com (M. Zhou).

0143-7208/$ - see front matter © 2007 Elsevier Ltd. All rights reserved.
doi:10.1016/j.dyepig.2007.04.002

oxidation. Pozzo et al. compared the cathodic production of hydrogen peroxide by a graphite electrode and a gas diffusion electrode; these researchers confirmed that the latter displayed higher selectivity for hydrogen peroxide production, although the main drawback of the cathode was its short lifetime due to the loss of dispersed graphite from the cathode [7]. Based on the above research results, it can be concluded that different cathodes possess unique electrochemical characteristics in terms of hydrogen peroxide production, which can lead to incompatible results. Furthermore, these electrochemical systems require modifications in order to be more suitable for practical waste water treatment. For example, current efficiency needs further enhancement over a much wider pH range especially in the case of AOPs so as to reduce treatment costs and the cathode system requires simplification to be more convenient and easier for scaling-up. If these problems can be overcome to a certain extent, hydrogen peroxide production *in situ* would be expected to be an economical method and thus its environmental application would be greatly enhanced.

Therefore, in this work, modifications have been made to develop an efficient undivided electrochemical system for environmental application, using a cathode system which employed gas sparging directly instead of common gas diffusion which could be readily scaled-up as gas sparging enjoys extensive use in environmental engineering. One notable advantage of the undivided system employed was its high current efficiency for hydrogen peroxide production over the pH range 3–11. Cathode preparation, as well as electrochemical properties and stability towards hydrogen peroxide production were investigated in the context of the feasibility of using the electrochemical system for organic waste water treatment using the azo dye, C.I. Acid Red 2, as a model pollutant. Key parameters such as electrolyte concentration, pH, cathodic potential and Fe^{2+} concentration were studied. The particular dye was selected because it is very difficult to decompose using traditional processes and thus constitutes a serious environmental problem [9,10] and also, because relatively few papers have appeared on azo dye waste water treatment [11] although indirect electrochemical oxidation had been extensively investigated for the treatment of other organic pollutants [8,12,13] including pesticides [14,15].

2. Experimental

2.1. Reagents and chemicals

Polytetrafluoroethylene (PTFE) (60%, 3F New Materials Co. Ltd, Shanghai, China) was used as received for cathode preparation. C.I. Acid Red 2 (methyl red) was purchased from Fisher Scientific Worldwide Company, Hong Kong; its structure is shown in Fig. 1. The activated carbon and graphite powder were obtained from Shanghai Reagents Co.; all other chemicals including anhydrous Na_2SO_4, H_2SO_4, NaOH, $FeSO_4$ and ethanol were of analytical grade.

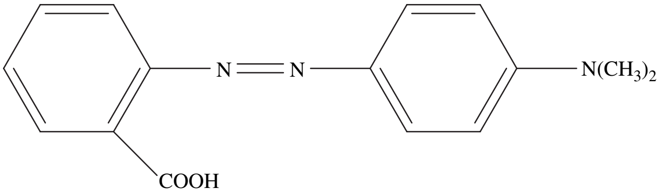

Fig. 1. Structure of methyl red.

2.2. Cathode preparation

An appropriate amount of graphite powder (or carbon black) and PTFE dispersion were mixed in an ultrasonic bath for 10 min at room temperature. Ethanol was added as solvent and mixing was continued at 80 °C until the mixture resembled an ointment in appearance. The resulting graphite (or carbon)–PTFE cake was pulverized to form a sheet of ~0.20 mm thickness which was then pressed onto a piece of stainless steel mesh under a pressure of 15 MPa for 3 min. Depending on requirement, the prepared electrode would be further calcined at 300 °C for 2 h. Finally, the electrode was immersed in acetone for 24 h to remove residual organic compounds such as ethanol and then rinsed in deionized water five times, followed by air drying.

2.3. Procedures

Fig. 2 shows the schematic setup of the electrochemical system. The experiments were conducted using a CHI600B

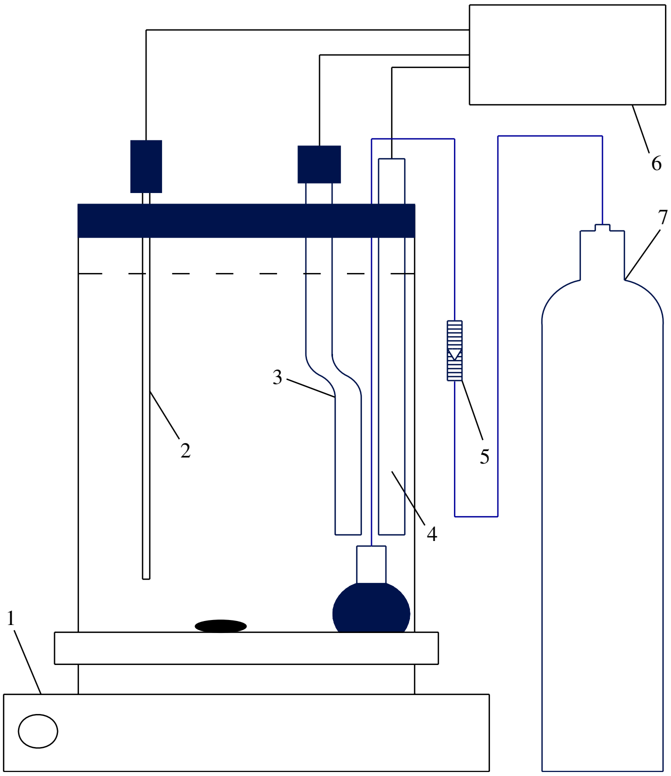

Fig. 2. Schematic diagram of experimental setup: (1) magnetic stirrer; (2) platinum wire; (3) saturated calomel electrode (SCE); (4) cathode; (5) gas flowmeter; (6) CHI600B; (7) oxygen tank.

electrochemical workstation (Shanghai Chenhua, China) in a conventional three-electrode cell at room temperature. The prepared cathode (1 cm^2 area) was selected as working electrode, a platinum wire electrode as counter electrode and a saturated calomel electrode (SCE) as reference electrode. The distance between the working electrode and counter electrode was 3 cm.

The experiments for hydrogen peroxide generation were performed in an undivided cell of 100 mL capacity using constant magnetic stirring. The solution comprised Na_2SO_4 as supporting electrolyte and its pH was adjusted using H_2SO_4 or NaOH prior to electrolysis. Oxygen was sparged near the cathode at a desired flow rate. Once the power to the electrochemical workstation was turned on, the cathodic potential was adjusted to a suitable value. At certain time intervals, samples were taken and the electric charges were recorded.

The procedures for dye waste water decolorization were very similar, except that the solution used was model waste water, comprising certain amounts of C.I. Acid Red 2 and supporting electrolyte, Na_2SO_4.

2.4. Analytical methods

Cyclic voltammetry (CV) was employed to confirm and compare hydrogen peroxide generation under specific conditions. CV was recorded using a CHI600B electrochemical workstation at a scan rate of 50 mV/s using the three-electrode cell described previously. Hydrogen peroxide concentration was determined spectrophotometrically using the potassium titanium(IV) oxalate method ($\lambda = 402$ nm) [16]. The current efficiency (CE) for hydrogen peroxide generation is defined as follows [6]:

$$\mathrm{CE} = \frac{nFC_{\mathrm{H_2O_2}}V}{\int_0^t I\,\mathrm{d}t} \times 100\% \tag{2}$$

where n is the number of electrons transferred for oxygen reduction to H_2O_2, F is the Faraday constant (96486 C/mol), $C_{\mathrm{H_2O_2}}$ the concentration of H_2O_2 (mol/L), V the bulk volume (L), I the applied current (A), and t is time (s).

Dye concentration was determined spectrophotometrically using a (Techcomp 8500, Shanghai) UV–visible spectrophotometer at $\lambda = 523$ nm and decolorization efficiency (η) was calculated using Eq. (3):

$$\eta = \frac{A_0 - A_t}{A_0} \times 100\% \tag{3}$$

where, A_0 and A_t are the absorbances of the dye waste water initially and at time t, respectively. A Hitachi S-4700 scanning electron microscope was used to record SEM images of the cathode.

3. Results and discussions

3.1. Cathode preparation

3.1.1. Choice of cathode materials

It is apparent that cathode materials affect the performance of hydrogen peroxide production notably. Fig. 3 shows the CV for oxygen reduction at the different carbon and graphite electrodes, respectively. It was seen that the latter had an obvious current response for hydrogen peroxide production, which showed a peak current density of 7.1 mA/cm^2 at a cathodic potential of −0.55 V vs. SCE. This outcome was similar to the cathodic potential for hydrogen peroxide production [17]. In a basic medium, hydrogen peroxide exists predominantly as the hydroperoxide ion, which is supposed to be generated according to Eq. (4):

$$O_2 + H_2O + 2e^- \rightarrow HO_2^- + OH^- \tag{4}$$

Therefore, graphite was adopted as the material for the catalytic layer in cathode preparation.

3.1.2. Effect of the mass ratios of graphite:PTFE

PTFE in the cathode serves two functions namely to bind the high surface carbon or graphite particles into a cohesive layer and to impart hydrophobic character to the layer. Table 1 lists the concentration of hydrogen peroxide and current efficiencies for different mass ratios of graphite:PTFE. Generally, a decrease of mass ratio is accompanied by a decrease in the effective sites for the electrochemical reaction of hydrogen peroxide production. However, a higher PTFE content makes the layer more hydrophobic, minimizing cathode flooding and facilitating gas distribution, as a consequence of which, the reaction opportunity of dioxygen electrochemical reduction improves. As the production of hydrogen peroxide depends on the active area and gas diffusion ability of the

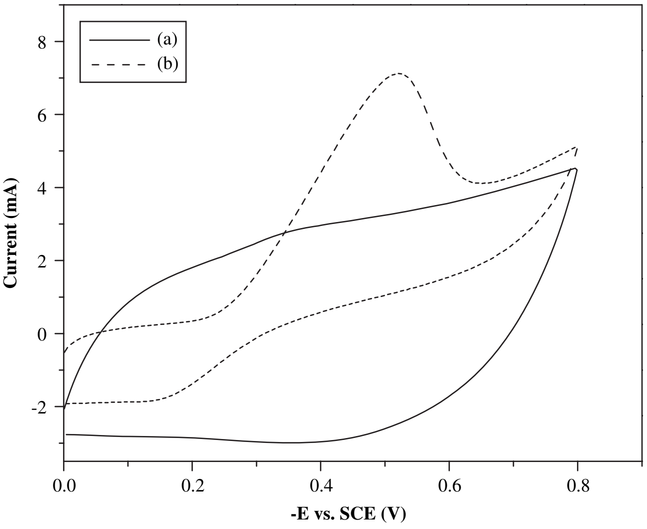

Fig. 3. Cyclic voltammetry of oxygen reduction on the cathodes made by different materials: (a) carbon and (b) graphite. Conditions: Na_2SO_4 0.1 M, pH 13.2, oxygen flow rate 0.4 L/min, scan rate 50 mV/s.

Table 1
Influence of mass ratios of graphite to PTFE on H_2O_2 accumulation and current efficiency

	$C_{H_2O_2}$ (mg/L)			CE (%)		
	20 min	40 min	60 min	20 min	40 min	60 min
1:1	1.74	1.82	2.94	12.7	8.90	8.05
2:1	29.8	54.7	74.3	78.3	75.3	70.1
3:1	7.88	14.9	20.8	38.3	35.9	31.5
4:1	2.89	3.6	4.90	26.3	21.1	22.8

Conditions: pH: 13.2; Na_2SO_4: 0.1 M; cathodic potential: −0.55 V vs. SCE; oxygen flow rate: 0.4 L/min.

cathode, the aforementioned two adverse aspects result in an optimal mass ratio of graphite:PTFE.

In terms of theoretical analysis, it was observed that a mass ratio of 2:1 gave the best performance in terms of both hydrogen peroxide generation and current efficiency. At such a mass ratio, the hydrogen peroxide concentration reached 74.3 mg/L after 60 min, and current efficiency was 70.1%, although this was a decrease from that of 78.3% after 20 min.

The hydrogen peroxide concentration increased with increasing time while the current efficiency declined. Furthermore, higher concentrations of hydrogen peroxide led to the large decline of current efficiency with time, the reasons for which are complicated. Qiang et al. investigated the stability of hydrogen peroxide and concluded that it decomposes rapidly with increasing pH especially at $pH > 9$ [6]. At high pH, HO_2^- would be the major species, which catalyzes hydrogen peroxide decomposition as suggested by Abel [18]:

$$HO_2^- + H_2O_2 \rightarrow H_2O + O_2 + OH^- \tag{5}$$

We speculate that this behavior might also occur in the present work especially in alkaline solution so that higher concentrations of hydrogen peroxide produce rapid decomposition, which causes a reduction in current efficiency with increasing time.

3.1.3. Effect of calcination temperature

Fig. 4 shows the accumulation of hydrogen peroxide with and without calcination during electrode preparation. It was found that the concentration of hydrogen peroxide increased during the initial 100 min but after 120 min the accumulated hydrogen peroxide reached steady-state concentrations and thereafter remained almost constant. Brillas et al. observed similar phenomenon which was attributed to the balance of generation and decomposition of peroxide [19]. Besides the self-decomposition described above, hydrogen peroxide, anodic oxidation might also be responsible for decomposition [8]:

$$H_2O_2 \rightarrow HO_2^{\bullet} + H^+ + e^- \tag{6}$$

$$HO_2^{\bullet} \rightarrow O_2 + H^+ + e^- \tag{7}$$

After 140 min, the concentration of hydrogen peroxide without calcination treatment was ∼99.9 mg/L, compared to ∼97.4 mg/L in the case of calcined electrode. Thus the hydrogen peroxide accumulation without calcination was higher than that with calcination, but the difference was insignificant. These results can be attributed to the surface characteristics of the two electrodes. As shown in Fig. 5, the surface of the uncalcined cathode was smooth and flat; no obvious white grains could be identified, indicating that the PTFE and graphite had been blended well [20]. It seemed that the structure of the electrode surface after calcination did not change greatly except for the presence of macropores which may have enabled the solution to be more easily transported to the electrode, which thus hindered gas diffusion and, thereby, the generation of hydrogen peroxide was relatively reduced. Hence, in the following experiments, the electrode was not calcined.

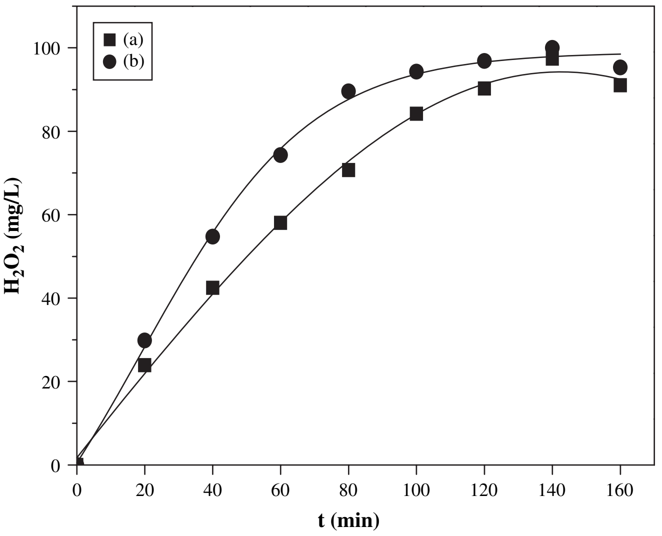

Fig. 4. Effect of temperature on hydrogen peroxide accumulation: (a) after calcination; (b) without calcination. Conditions: Na_2SO_4 0.1 M, pH 13.2, cathodic potential −0.55 V (vs. SCE), oxygen flow rate 0.4 L/min.

Furthermore, as shown in Fig. 4, the average hydrogen peroxide generation rate after 2 h was >45 mg/L/h/cm^2 (cathode area). This hydrogen peroxide production performance was greatly improved compared with the literature [21,22]. Forti et al. used an azobenzene-modified, oxygen-fed, graphite/PTFE electrode and observed hydrogen peroxide generation rate of ∼34.2 mg/L/h/cm^2 [21] while Guillet et al., using a gas diffusion electrode modified with CoTMPP, found that using 0.2% Co content, the hydrogen peroxide generation rate was ∼10.2 mg/L/h/cm^2 [22].

3.2. Electrochemical characteristics

3.2.1. Electrochemical activity

Table 2 shows the H_2O_2 accumulation and current efficiency at 40 C under different conditions. In the case of no oxygen supply, pure nitrogen was bubbled into the solution for 15 min before electrolysis to guarantee oxygen-free conditions. It was confirmed that the supply of oxygen was a prerequisite for hydrogen peroxide generation. With increasing oxygen flow rate, both the concentration of hydrogen peroxide and current efficiency increased. However, when the flow rate reached 0.4 L/min, the promotion was small. Some researchers

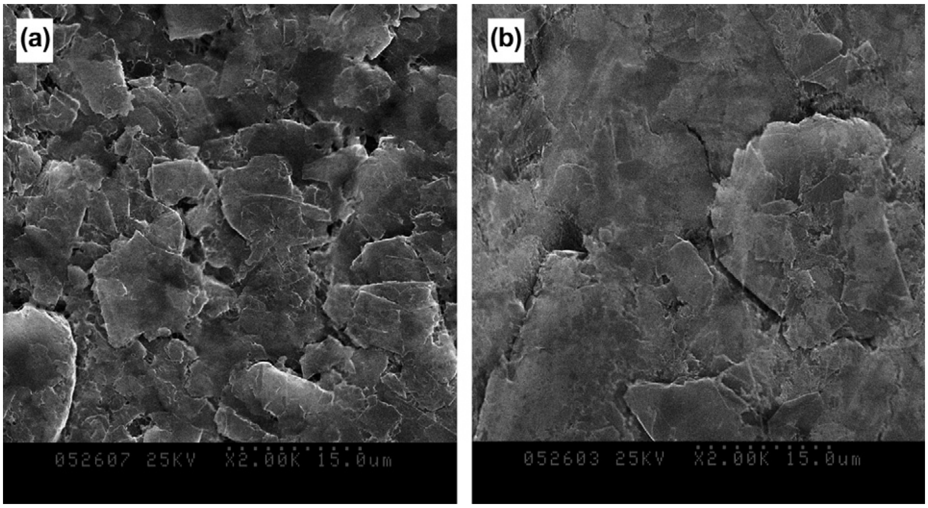

Fig. 5. Scanning electronic micrographs (SEM) of cathodes: (a) after calcination; (b) without calcination.

have indicated that further increase in oxygen flow rate after the optimal value did not enhance hydrogen peroxide production [6].

As shown in Table 2, the cathodic potential at -0.55 V showed best hydrogen peroxide generation and current efficiency. To disclose this tendency, a linear scanning voltammetry over wide cathodic potentials (0 to -1.5 V vs. SCE) was carried out (the results are not shown). Three peaks were observed, indicating three different reactions. The first peak appeared at -0.55 V vs. SCE, which was confirmed to be the generation of hydrogen peroxide while the second peak appeared at around -0.90 V vs. SCE and the third one at ~ -1.4 V vs. SCE. According to the literature [23,5], the two latter peaks are probably due to the reduction of oxygen to H_2O, and the formation of hydrogen. These side reactions at the cathode are as follows:

$$O_2 + 4H^+ + 4e^- \rightarrow 2H_2O \tag{8}$$

$$2H^+ + 2e^- \rightarrow H_2 \tag{9}$$

It was observed that a more positive cathodic potential produced a significant decrease in current density. Therefore, at a cathodic potential more positive than -0.55 V vs. SCE (e.g., -0.3 V), although the current efficiency was still relatively high the current response for hydrogen peroxide generation was small, which led to an unacceptable reaction time. More negative cathodic potentials would result in side electrochemical reactions, which result in reduced current density. Hence to achieve both good current efficiency and high hydrogen peroxide production, it is vital to maintain a suitable cathodic potential, for which, -0.55 V represents the best compromise.

The solution pH influenced the generation of hydrogen peroxide greatly. In acidic medium, the main reaction taking place is Eq. (1), while under alkaline conditions the reaction would be Eq. (4) as described above. Therefore, lower pH values (e.g., $pH < 3$) or higher pH values ($pH > 7$) will lead to the high production of hydrogen peroxide [6,17,24]; this work confirmed this. It was reported that hydrogen peroxide production and current efficiency were better at extreme acidic conditions ($pH < 2$) while at elevated pH the performance is markedly reduced [6,17]. However, in this work, the current efficiency was maintained at >61% within the investigated pH range. At pH 3, the hydrogen peroxide concentration and current efficiency were relatively higher, i.e., the current efficiency was at around 75.9%, which would benefit AOPs that performed best at $pH \sim 3$. Furthermore, in the present work, gas was sparged directly from the bottom of the undivided cell, which simplified the setup and thus might offer promise for environmental application.

Table 2
Electrochemical activity for H_2O_2 accumulation and current efficiency

No.	O_2 flow rate (L/min)	Cathodic potential (V)	pH	$C_{H_2O_2}$ (mg/L)	CE (%)
1	0	−0.55	3	–[a]	–
2	0.2	−0.55	3	26.8	38.0
3	0.4	−0.55	3	53.5	75.9
4	0.6	−0.55	3	57.1	81
5	0.4	−0.3	3	40.7	57.8
6	0.4	−0.7	3	39.4	55.9
7	0.4	−0.8	3	33.7	47.8
8	0.4	−0.55	5	43.2	61.3
9	0.4	−0.55	7	51.4	72.9
10	0.4	−0.55	11	55.1	78.2

[a] Not detected.

3.2.2. Electrochemical stability

To investigate the feasibility of such a system, the stability of the cathode for hydrogen peroxide generation was examined. As shown in Fig. 6, the decline in hydrogen peroxide and current efficiency were both insignificant. After 10 times reuse, current efficiency dropped from the original 75.9% to 73.7%, indicating a decay of 3.0%. This fact indicates that the present system would be useful for waste water treatment,

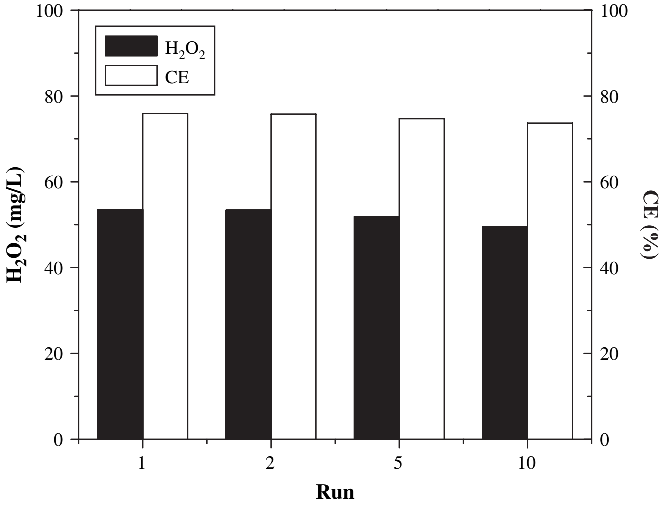

Fig. 6. Stability of the cathode. Conditions: Na_2SO_4 0.1 M, pH 3, cathodic potential −0.55 V (vs. SCE), oxygen flow rate 0.4 L/min.

and thus it was applied to dye waste water treatment in the section below.

3.3. Decolorization behavior

3.3.1. Effect of pH

Fig. 7 shows that low pH favored dye removal. With respect to pH 3, the decolorization efficiency reached 57% after 20 min. To validate the effectiveness of oxidation by hydrogen peroxide generated *in situ*, the extent of decolorization achieved using the external addition of a similar hydrogen peroxide concentration of 30 mg/L was studied at pH 3. It was found that decolorization was only 33.5% after 20 min, which was much lower than that secured using electrochemical generation. This finding may be attributed to the higher activity of hydrogen peroxide generated *in situ*. However, at pH 7 and 5, it reached only 35% and 29%, respectively. This is consistent with the concentration of hydrogen peroxide generated at different pH although the decolorization rate was found to slow down especially after 20 min treatment.

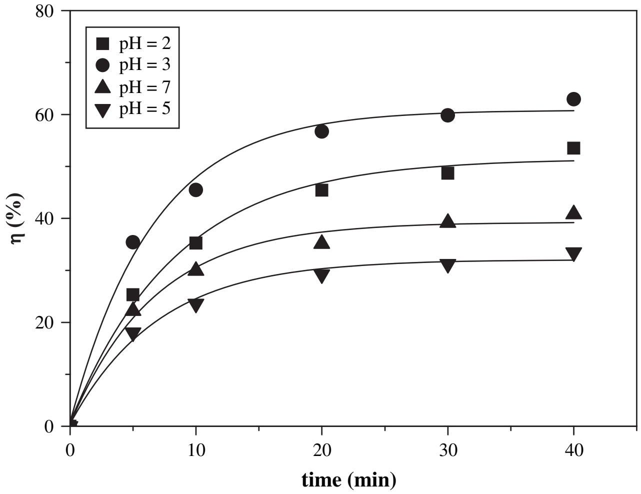

Fig. 7. Influence of pH on decolorization. Conditions: cathodic potential −0.55 V vs. SCE, Na_2SO_4 0.1 M, initial methyl red 100 mg/L, oxygen flow rate 0.4 L/min.

To explore the possible mechanism, the absorption spectra of dye degradation were investigated, as shown in Fig. 8. It was observed that before treatment the dye was characterized by one main band in the visible region with a peak at 523 nm, and two bands in the ultraviolet region situated at around 290 and 215 nm. After 20 min degradation, the absorbance of the remaining solution in the visible region decreased quickly, while simultaneously the absorbances at 290 and 215 nm increased, indicating that the azo bond was destroyed and degradative intermediates were generated. The rapid decolorization of the dye can be attributed to the initial electrophilic cleavage of the azo bonds attached to the constituent benzene ring. After 40 min, the absorbance in the visible region fell slightly, but the absorbance in the UV region increased, indicating that the degradation intermediates further increased but did not decompose. From the above results, it was clear that dye decolorization was a rapid process but the destruction of the benzene ring was difficult [25]. This also implies that the electro-generated hydrogen peroxide was too weak to further break the generated intermediates containing aromatic rings. The diminution of the dye and the generation of intermediates are competitive reactions, which led to the azo bond being broken very slowly after 20 min treatment.

3.3.2. Effect of cathodic potential

Fig. 9 shows that at −0.55 V vs. SCE, dye removal was highest at 60% after 30 min, due to H_2O_2 production being optimum at −0.55 V vs. SCE. When the cathodic potential was further increased to −0.7 and −0.8 V vs. SCE, the possibility of side reactions increased and hydrogen peroxide production decreased, causing dye decolorization to fall.

3.3.3. Effect of Na_2SO_4 concentration

In dye waste water, electrolyte contents can be very high; in this work, Na_2SO_4 was selected as model electrolyte. It was found (Fig. 10) that after 10 min treatment the decolorization efficiency was 25.7% at 0.05 M Na_2SO_4, while at 0.075 and 0.2 M Na_2SO_4 it reached 35.6% and 49.3%, respectively. Thus as the Na_2SO_4 concentration increased, greater decolorization efficiency was achieved. The increasing Na_2SO_4 concentration enhanced current density at the same cathodic potential, which promoted the production of electro-generated H_2O_2. Therefore, greater decolorization efficiency was achieved at higher electrolyte concentrations. Since the decolorization enhancement of 0.1 M and 0.2 M Na_2SO_4 was not marked, this process can be effective for the treatment of waste water of moderate electrolyte content. The results also indicated that the background ionic strength in waste water could be directly used as a supporting electrolyte for hydrogen peroxide generation *in situ*.

3.3.4. Effect of initial dye concentration

Fig. 11 shows that when the initial concentration was 25 mg/L, the dye was almost decolorized after 40 min. With

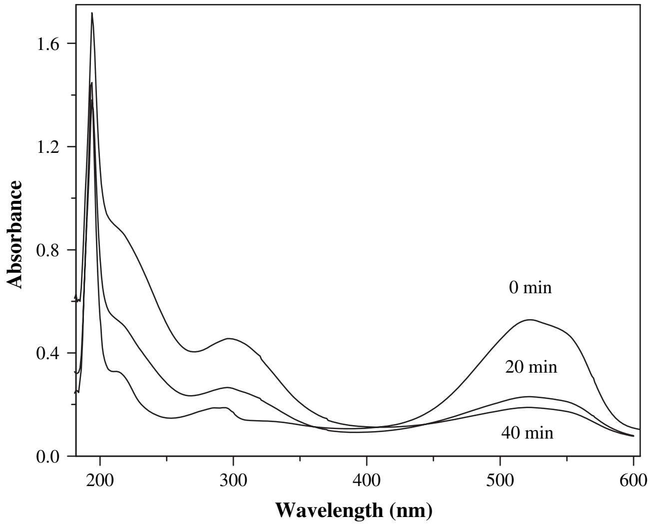

Fig. 8. The absorption spectra of methyl red degradation at a typical time. Conditions: pH 3.0, cathodic potential −0.55 V vs. SCE, Na_2SO_4 0.1 M, initial methyl red 100 mg/L, oxygen flow rate 0.4 L/min.

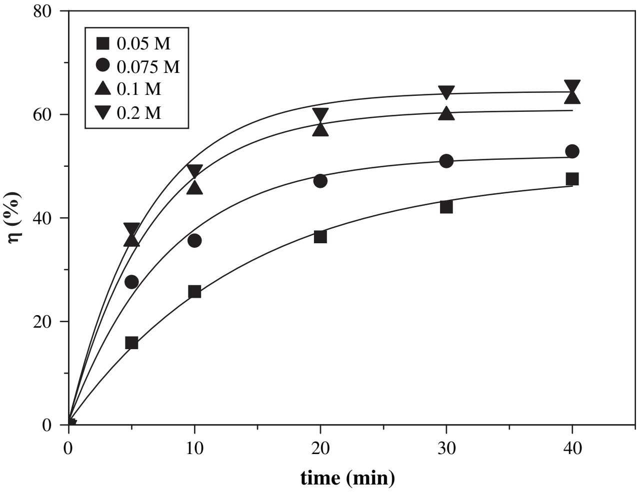

Fig. 10. Influence of Na_2SO_4 concentration on decolorization. Conditions: pH 3.0, cathodic potential −0.55 V, initial methyl red 100 mg/L, oxygen flow rate 0.4 L/min.

increase in dye concentration from 50 to 100 mg/L, the decolorization efficiency decreased from 84% to 63%. Although the decolorization efficiency decreased with initial methyl concentration, the absolute removal of the dye increased. For example, the dye decolorization increased from 42 to 63 mg/L when the initial dye concentration increased from 50 to 100 mg/L implying that within the concentration range used, the process favored the decolorization of the dye.

3.3.5. Effect of Fe^{2+} concentration

Fig. 12 shows the effect of the ferrous concentration on color removal after 20 min treatment. In the presence of ferrous ions, powerful hydroxyl radicals would be generated by the following Fenton reaction:

$$Fe^{2+} + H_2O_2 + H^+ \rightarrow Fe^{3+} + {}^{\bullet}OH + H_2O \qquad (10)$$

Thus the process turned into the so-called electro-Fenton process, and an obvious promotion of color removal was observed. In the absence of Fe^{2+}, the color removal was around 56%, which increased significantly to 79% when the concentration of $Fe^{2+}$was increased to 0.2 mM. However, further increase in the concentration of ferrous ions above this point did not bring about further improvement in dye removal. It has been reported that an excess of ferrous ion would consume hydroxyl radicals, which would account for the observed decrease in dye removal [26].

$$Fe^{2+} + {}^{\bullet}OH \rightarrow Fe^{3+} + OH^- \qquad (11)$$

These facts confirm that a suitable concentration of ferrous ion is an important prerequisite in the electro-Fenton process.

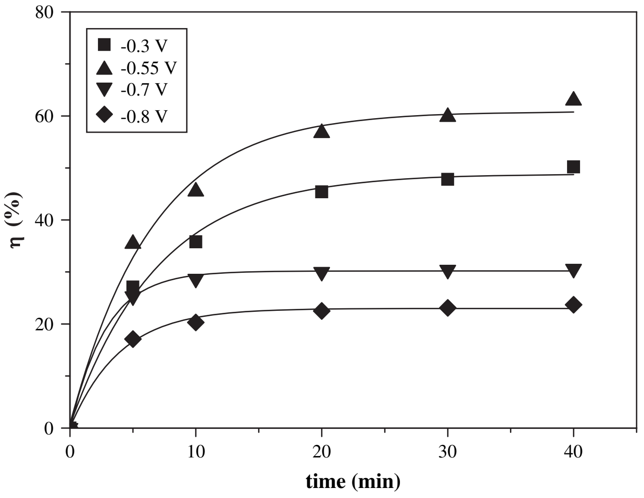

Fig. 9. Influence of cathodic potential on decolorization. Conditions: pH 3.0, Na_2SO_4 0.1 M, cathodic potential −0.55 V vs. SCE, initial methyl red 100 mg/L, oxygen flow rate 0.4 L/min.

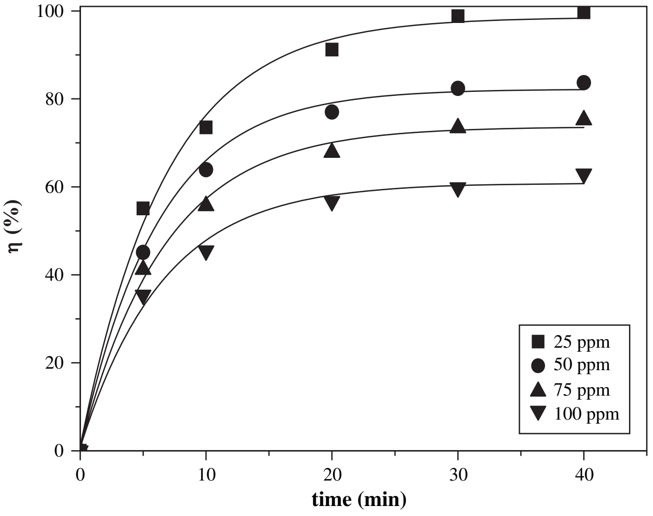

Fig. 11. Influence of the initial methyl red on decolorization. Conditions: pH 3.0, cathodic potential −0.55 V vs. SCE, Na_2SO_4 0.1 M, oxygen flow rate 0.4 L/min.

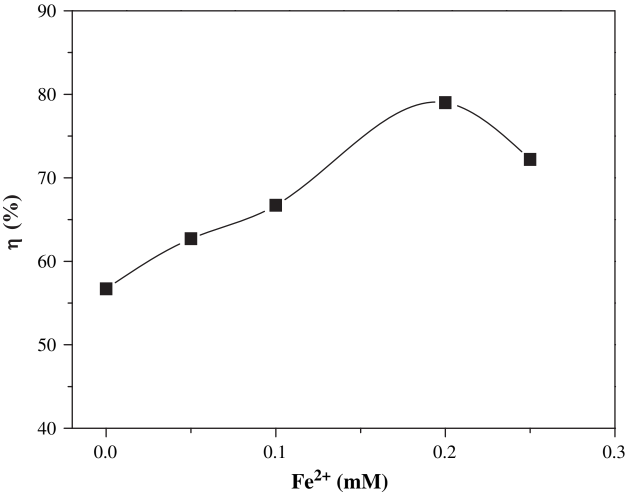

Fig. 12. Influence of Fe^{2+} concentration on decolorization. Conditions: pH 3.0, Na_2SO_4 0.1 M, cathodic potential −0.55 V, initial methyl red 100 mg/L, oxygen flow rate 0.4 L/min.

4. Conclusions

It was found that high hydrogen peroxide production was obtained when the cathode was prepared using a mass graphite:PTFE ratio of 2:1 without calcination. The cathode performed well for H_2O_2 production and current density. Within the investigated pH range (3–11), H_2O_2 concentration could reach >43 mg/L per 1 cm^2 electrode area at a cathodic potential of −0.55 V vs. SCE and the current density could reach as high as 78%. The pH influenced dye degradation, with pH 3 being optimum. Decolorization efficiency increased with Na_2SO_4 concentration and the presence of ferrous ion enhanced decolorization, with an optimal concentration being 0.20 M.

Acknowledgments

We would like to acknowledge financial supports of this work provided by the National Science Foundation of China (no. 20306027 and 20676121), the Science Foundation of Zhejiang Province (no. Y504129) and Pao's Scholarship.

References

[1] Comninellis Ch, Pulgarin C. Anodic oxidation of phenol for waste water treatment. J Appl Electrochem 1991;21:703–8.

[2] Bunce NJ, Merica SG, Lipkowski J. Prospects for the use of electrochemical methods for the destruction of aromatic organochlorine wastes. Chemosphere 1997;35:2719–26.

[3] Chen XM, Chen GH, Gao FR, Yue PL. High-performance Ti/BDD electrodes for pollutant oxidation. Environ Sci Technol 2003;37:5021–6.

[4] Zhou MH, Dai QZ, Lei LC, Ma C, Wang D. Long life modified lead dioxide anode for organic waste water treatment: electrochemical characteristics and degradation mechanism. Environ Sci Technol 2005;39:363–70.

[5] Alvarez-Gallegos A, Pletcher D. The removal of low level organics via hydrogen peroxide formed in a reticulated vitreous carbon cathode cell. Part 1. The electrosynthesis of hydrogen peroxide in aqueous acid solutions. Electrochim Acta 1998;44:853–61.

[6] Qiang ZM, Chang JH, Huang CP. Electrochemical generation of hydrogen peroxide from dissolved oxygen in acidic solutions. Water Res 2002;36:85–94.

[7] Pozzo AD, Palma LD, Merli C, Petrucci E. An experimental comparison of a graphite electrode and a gas diffusion electrode for the cathodic production of hydrogen peroxide. J Appl Electrochem 2005;35:413–9.

[8] Brillas E, Bastida RM, Liosa E, Casado J. Electrochemical destruction of aniline and 4-chloroaniline for waste water treatment using a carbon–PTFE-fed cathode. J Electrochem Soc 1995;142:1733–41.

[9] Dai QZ, Zhou MH, Lei LC. Wet electrolytic oxidation of cationic red X-GRL. J Hazard Mater 2006;137:1870–4.

[10] Kusvuran E, Irmak S, Yavuz HI, Samil A, Erbatur O. Comparison of the treatment methods' efficiency for decolorization and mineralization of reactive black 5 azo dye. J Hazard Mater 2005;119:109–16.

[11] Wang AM, Qu JH, Ru J, Liu HJ, Ge JT. Mineralization of an azo dye acid red 14 by electro-Fenton's reagent using an activated carbon fiber cathode. Dyes Pigments 2005;65:227–33.

[12] Oturan MA, Peiroten J, Chartrin P, Acher AJ. Complete destruction of *p*-nitrophenol in aqueous medium by electro-Fenton method. Environ Sci Technol 2000;34:3474–9.

[13] Wu ZC, Zhou MH, Wang DH. Synergetic effects of anodic–cathodic electrocatalysis for phenol degradation in the presence of iron(II). Chemosphere 2002;48:1089–96.

[14] Oturan MA, Aaron JJ, Oturan N, Pinson J. Degradation of chlorophenoxyacid herbicides in aqueous media, using a novel electrochemical method. Pestic Sci 1999;55:558–62.

[15] Ventura A, Jacquet G, Bermond A, Camel V. Electrochemical generation of the Fenton's reagent: application to atrazine degradation. Water Res 2002;36:3517–22.

[16] Sellers RM. Spectrophotometric determination of hydrogen peroxide using potassium titanium(IV) oxalate. Analyst 1980;150:950–4.

[17] Hsiao YL, Nobe K. Oxidative reactions of phenol and chlorobenzene with in situ electrogenerated Fenton's reagent. Chem Eng Commun 1993;126:97–110.

[18] Abel E. Uber die selbstzersetzung von wasserstoffsuperoxyd. Monatsh Chem 1952;83:422–39.

[19] Brillas E, Calpe JC, Casado J. Mineralization of 2, 4-D by advanced electrochemical oxidation processes. Water Res 2000;34:4509–14.

[20] Shen ZM, Yang J, Hu XF, Lei YM, Ji XL, Jia JP, et al. Dual electrodes oxidation of dye waste water with gas diffusion cathode. Environ Sci Technol 2005;39:1819–26.

[21] Forti JC, Nunes JA, Lanza MRV, Bertazzoli R. Azobenzene-modified oxygen-fed graphite/PTFE electrodes for hydrogen peroxide synthesis. J Appl Electrochem 2007;37:527–32.

[22] Guillet N, Roué L, Marcotte S, Viliers D, Dodelet JP, Chhim N, et al. Electrogeneration of hydrogen peroxide in acid medium using pyrolyzed cobalt-based catalysts: influence of the cobalt content on the electrode performance. J Appl Electrochem 2006;36:863–70.

[23] Xu J, Huang WH, McCreery RL. Isotope and surface preparation effects on alkaline dioxygen reduction at carbon electrodes. J Electroanal Chem 1996;410:235–42.

[24] Sudoh M, Kitaguchi H, Koide K. Electrochemical production of hydrogen peroxide by reduction of oxygen. J Chem Eng Jpn 1985;18:409–14.

[25] Solozhenko EG, Soboleva NM, Goncharuk VV. Decolourization of azo dye solutions by Fenton's oxidation. Water Res 1995;29:2206–10.

[26] Panizza M, Cerisola G. Removal of organic pollutants from industrial waste water by electrogenerated Fenton's reagent. Water Res 2001;35:3987–92.